

Supplementary materials

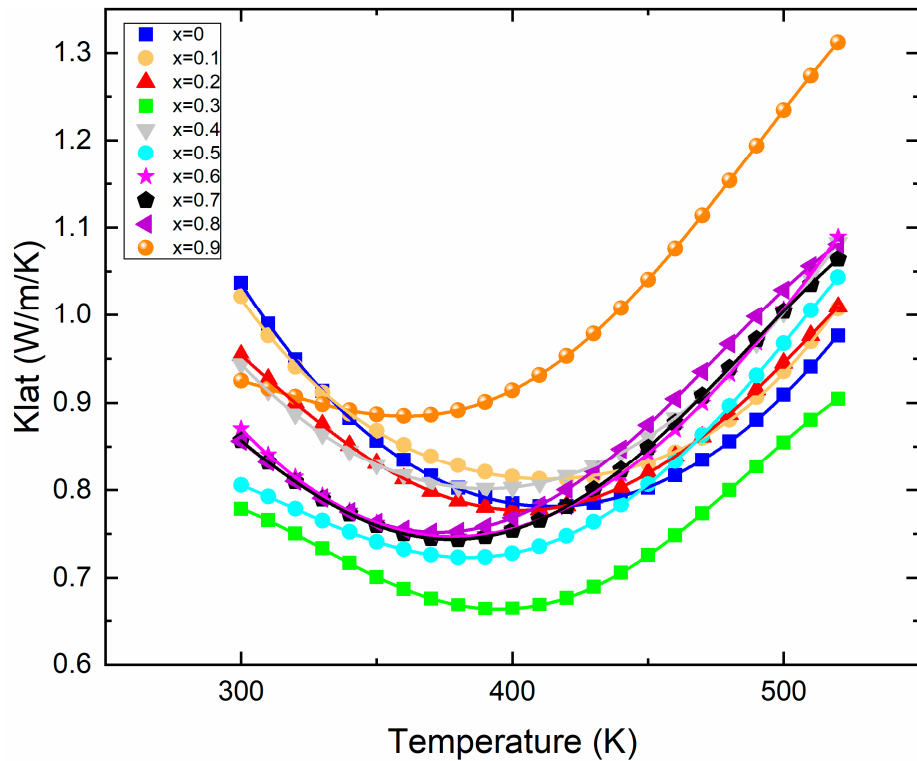


Figure S1 : Lattice component of the total thermal conductivity of $\text{Bi}_{2-x}\text{Sb}_x\text{Te}_3$ as a function of temperature

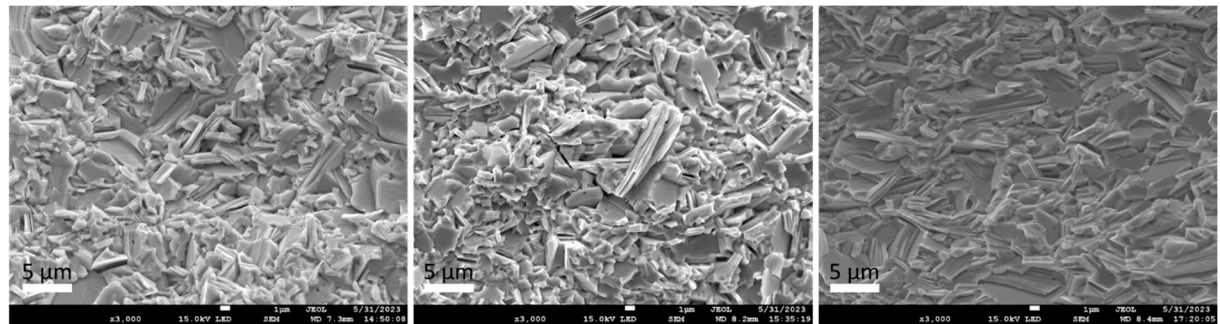


Figure S2 : SEM Picture of broken ingots of S1 (left), S2 (center) and S3 (right), using the same magnification, looking perpendicularly to the pressing direction. No clear difference can be seen between S1 and S2. The S3 sample shows the onset of slight alignment of the grains.

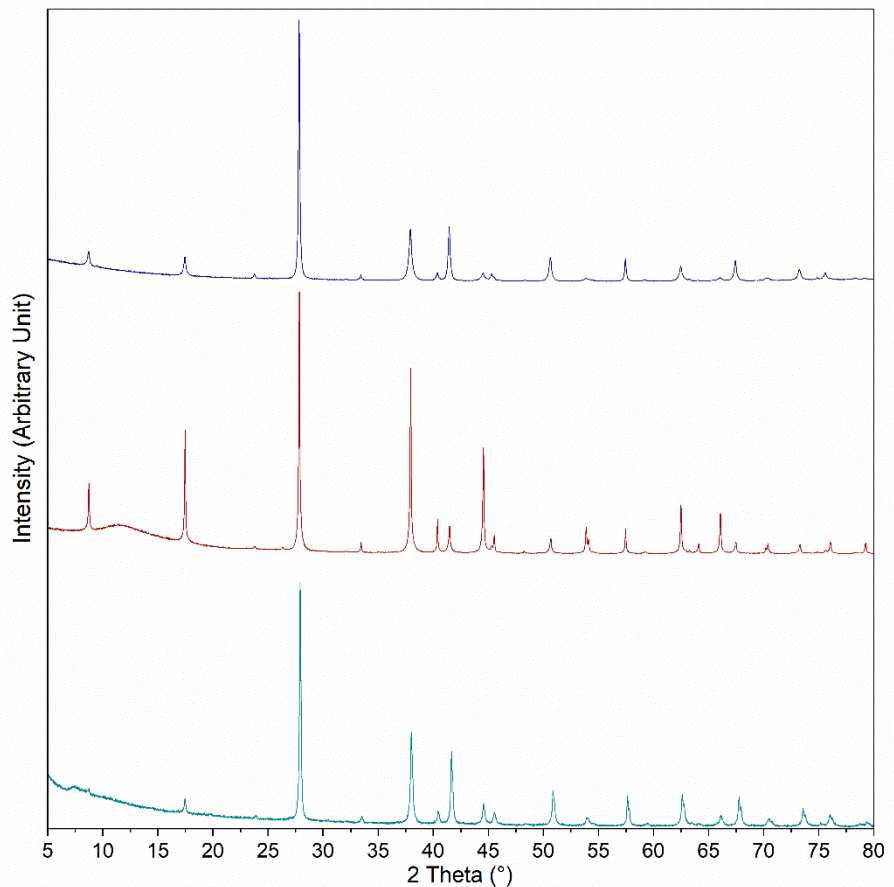


Figure S3 : powder diffraction patterns of $\text{Bi}_{1.5}\text{Sb}_{0.5}\text{Te}_3$ (R-3m space group, Te1 (0, 0, 0) – Te2 (0, 0, z) – Bi/Sb (0, 0, z')) acquired in three different ways, top: height of the cylindrical puck (parallel to the pressing direction) middle: surface of the cylindrical puck (perpendicular to the pressing direction); bottom: crushed powder after SPS

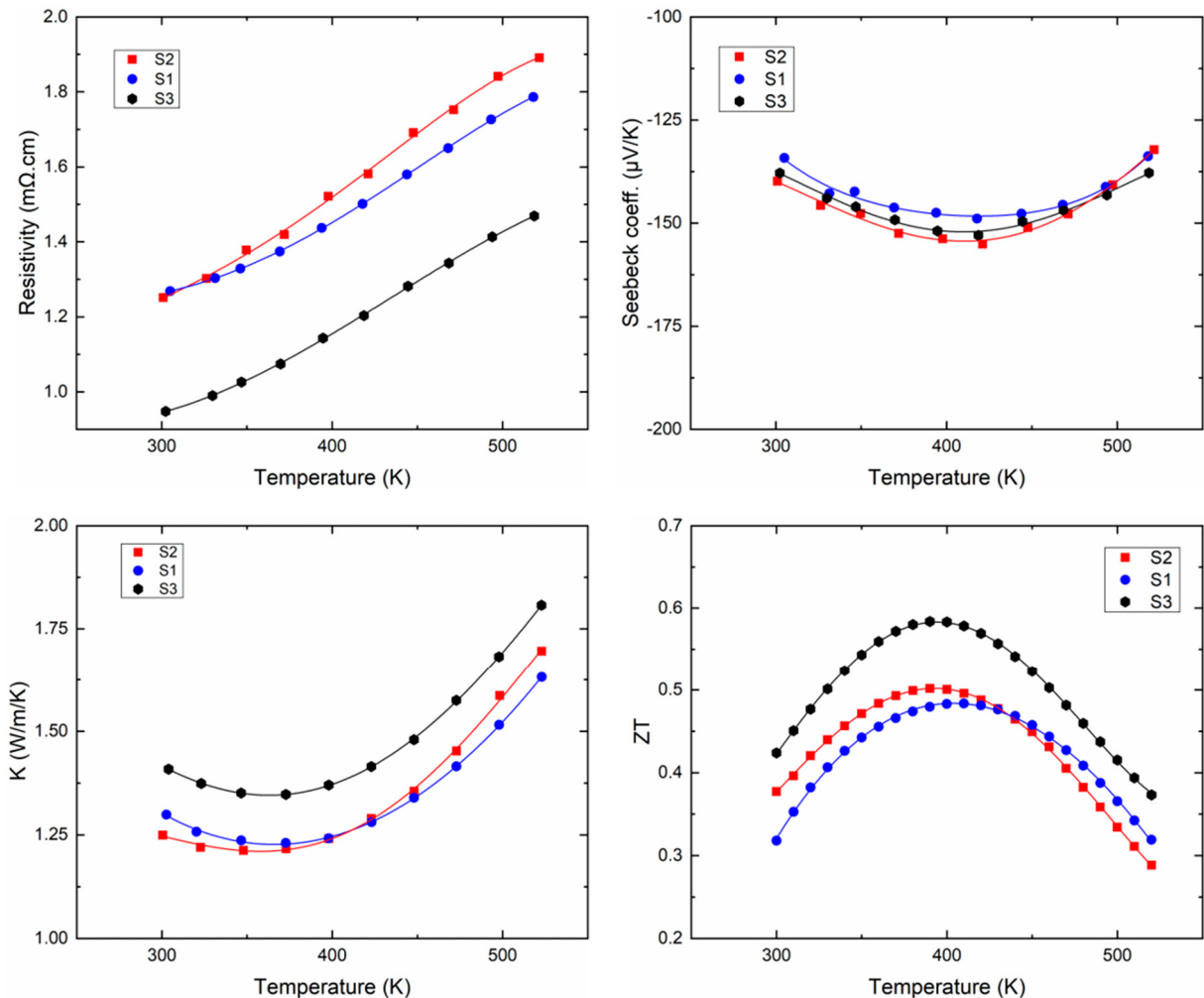


Figure S4: Transport properties and thermoelectric figure of merit of the samples S1, S2 and S3.

Table S1: Other crystallographic parameters deduced by the Rietveld modeling. Atomic coordinates Te1 (0, 0, 0) – Te2 (0, 0, z) – Bi1 (0, 0, z’)

	Bi ₂ Te ₃	Bi _{1.9} Sb 0.1Te ₃	Bi _{1.8} Sb 0.2Te ₃	Bi _{1.7} Sb 0.3Te ₃	Bi _{1.6} Sb 0.4Te ₃	Bi _{1.5} Sb ₀ . 5Te ₃	Bi _{1.4} Sb 0.6Te ₃	Bi _{1.3} Sb 0.7Te ₃	Bi _{1.2} Sb 0.8Te ₃	Bi _{1.1} Sb 0.9Te ₃
Space group: R-3m (n°166)										
a	4.387 26(4)	4.3855 0(5)	4.3796 4(5)	4.3730 1	4.3678 0(6)	4.3599 5(5)	4.3533 5(5)	4.3481 0(5)	4.3422 8(4)	4.3352 9(5)
c	30.48 02(4)	30.473 8(4)	30.482 2(4)	30.484 2(4)	30.492 2(4)	30.493 1(4)	30.494 8(4)	30.500 9(4)	30.505 8(4)	30.500 4(4)
Te1 - B _{iso})	0.90(9))	1.32(10))	1.35(9)	1.16(9)	1.29(10))	0.94(9)	1.34(9)	0.49(9)	0.53(8)	1.5(1)
Te2 - z	0.209 11	0.2093	0.2095 4	0.2102 4	0.2094	0.2102 1	0.2105 3	0.2102 2	0.2103 7	0.2095 9
Te2- B _{iso})	1.1(1)	1.5(1)	1.7(1)	1.9(1)	1.5(1)	1.0(1)	1.6(1)	0.41(10))	0.86(9)	1.2(1)
Bi1/Sb 1 – z’	0.400 56	0.4007 4	0.4005 7	0.4003 5	0.4004 2	0.3998 8	0.3998 7	0.3997 2	0.3998 6	0.3998
Bi1/Sb 1 - Biso)	1.29(6))	1.52(6)	2.10(7)	2.02(7)	2.00(8)	1.31(7)	1.97(7)	0.64(6)	0.67(5)	1.19(6)
Average apparent size (anisotropy):	540.2 300 (46.96 00)	526.78 00 (51.910 0)	514.44 00 (60.160 0)	507.95 00 (49.720 0)	504.13 00 (43.320 0)	528.18 00 (51.260 0)	483.75 00 (51.490 0)	527.42 00 (30.040 0)	583.24 00 (25.560 0)	514.62 00 (42.490 0)